Received: 20 January 2021 | Revised: 15 April 2021 | Accepted: 15 April 2021

DOI: 10.1002/pat.5355

RESEARCH ARTICLE

polymers for advanced technologies WILEY

The role of amphiphilic chitosan in hybrid nanocellulose–reinforced polylactic acid biocomposite

H. Nasution[1] | Niyi G. Olaiya[2] | M. K. Mohamad Haafiz[2] | C. K. Abdullah[2] | Suriani Abu Bakar[3] | Funmilayo G. Olaiya[1] | Azmi Mohamed[3] | Abdul Khalil H. P. S.[2]

[1]Department of Chemical Engineering, Faculty of Engineering, Universitas Sumatera Utara, Medan, 20155, Indonesia

[2]School of Industrial Technology, Universiti Sains Malaysia, Gelugor, 11800, Malaysia

[3]Nanotechnology Research Centre, Faculty of Science and Mathematics, Universiti Pendidikan Sultan Idris, Tanjong Malim, 35900, Malaysia

Correspondence
Abdul Khalil H. P. S. and N.G. Olaiya, School of Industrial Technology, Universiti Sains Malaysia, Gelugor, 11800 Penang, Malaysia.
Email: akhalilhps@gmail.com (A. K. H. P. S.); ngolaiya@futa.edu.ng (N. G. O.)

Funding information
Ministry of Education, Grant/Award Number: RUI/1001/PTEKIND8014119

Abstract

The blending of hydrophilic materials with hydrophobic polymers has been reported with agglomeration due to their functional group immiscibility properties. In this study, the properties of PLA/CNF biocomposite were enhanced with amphiphilic chitosan produced by a substitution reaction. The substitution reaction was studied with FT-IR analysis. The amphiphilic chitosan was used as part of the matrix PLA/chitosan and reinforced with CNF to obtain PLA/chitosan/CNF biocomposite using combined melt extrusion and compression molding technique. The morphology and structural bonding of amphiphilic chitosan added in the biocomposite were studied with SEM, XRD, and FT-IR. Furthermore, the mechanical, thermal, and wettability properties of PLA/chitosan/CNF composite were studied with tensile analysis, thermogravimetry analysis, differential scanning calorimetry, water absorption, thickness swelling, and contact angle test. The preparation of the amphiphilic chitosan was successful, as observed from the FT-IR functional group analysis. The PLA/chitosan/CNF biocomposite properties showed a significant enhancement in the miscibility, mechanical, and thermal properties with no agglomeration. The wettability test also showed that the composite has a reduced hydrophobic nature compared with the neat PLA. The PLA/chitosan/CNF properties showed potential use for packaging application.

KEYWORDS
amphiphilic, biocomposite, chitosan, nanocellulose reinforcement, polylactic acid

1 | INTRODUCTION

Biopolymer blends and reinforcement have been adapted for several applications.[1] This bio-based thermoplastics class is biodegradable and environmentally compostable, which is considered an advantage compared to synthetic polymers.[2] Researchers have conducted several studies on biopolymers with a major focus on their biodegradable and possible replacement for industrial application to reduce the environmental impact of synthetic polymers.[3,4] Several researchers in the environmental field have seen these as possible to close the carbon cycle through biodegradation.[5] Furthermore, biopolymers are novel materials in this century, and great importance is attached to them in the world of materials because of the future uncertainty of petroleum resources.[6,7]

Recently, biodegradable polymers have been developed for several industrial applications in biomedical, packaging, automobile, and so forth[8-10] The demand for biodegradable products increases as many policies have been developed to enhance its production due to environmental pollution.[11] Even though biodegradable polymers possess good biodegradable properties, other factors such as mechanical strength and toxicity have posed a challenge to their valorization. Therefore, studies on biopolymers are now focused on enhancing their properties with reinforcement to create material composites for several applications.[10,12] These studies are done with a focus on

retaining its biodegradability while deriving suitable properties.[12] Simultaneously, several climatic conditions have resulted from the pollution, which requires a fresh drive toward green materials. A calculated binary or ternary blends of biopolymers have been proposed as a bailout on the properties deficiencies of notable biopolymers such as PLA.[13,14]

Polylactic acid has been extensively studied for biodegradable composite because of its renewable feedstock.[15,16] PLA is classified as an aliphatic polyester and is commonly prepared from lactic acids.[17] PLA is often prepared from direct polymerization of lactic acid (polycondensation) or ring-opening polymerization lactide.[18] Lactic acid is often produced using the fermentation process.[19] Renewable resources such as corn, cassava, and sugarcane have been used for industrial preparation. Lactic acid is the simplest monomer of polylactic acid and a hydroxyl acid with an asymmetric carbon atom. Lactic acid has two optical configurations, D(+) lactic acid and L(−) lactic acid.[20] The first D (+) lactic acid is not common in animal sources, while L-isomer is common in mammals.[14,21] D(+) and L(−) configurations are produced in enzymatic (bacteria) systems. However, PLA is produced commercially using a fermentation process for economic reasons.[19]

Cellulose nanofiber has the challenge of miscibility with polylactic acid.[22] This majorly is due to the difference in their nature, that is, cellulose nanofiber is hydrophilic, while polylactic acid is hydrophobic. Poor miscibility between these two polymers has resulted in low mechanical properties from their blend.[23] PLA/CNF composite has been reported with agglomeration in the microstructure. This challenge often limits the quantity of cellulose nanofiber that can be added to the PLA matrix. The solution to the miscibility challenge of PLA with CNF has been proposed as novel research.[24]

Chitin is a polysaccharide from the exoskeleton of crustacea source, arthropods, mushrooms, nematodes, worms, diatoms, and insects.[25] The main sources of chitin are shellfish waste, such as crawfish shrimps, and crabs. It has been reported to be biocompatible, biodegradable, and nontoxic.[26] Deacetylated chitin is called chitosan with the white, hard, inelastic, and nitrogenous polysaccharide. Chitin is available for food supplements and skin treatment purposes. Worldwide, chitosan is the second most abundant and most important natural polysaccharide after cellulose. There are many chitosan derivatives; these include chitosan, *N*-acetyl chitosan, monoacetyl chitosan, di-butyryl chitosan, chitosan acetate, and so forth. The main derivative of chitosan is linear chitosan polymer of α (1 → 4) linked 2-amino-2-deoxy-β-D-glucopyranose and is easily derived N-deacetylation, to a varying degree that is characterized by the degree of deacetylation.[27,28] This is consequently a copolymer of *N*-acetyl glucosamine and glucosamine.[29]

Amphiphilic polymers are polymers with both hydrophilic and hydrophobic nature when mixed with other polymers.[28] Biopolymers such as chitosan exhibited such properties in their modified state. The amphiphilic properties of chitosan have been reported in the literature.[28,29] Several researchers have worked on blending amphiphilic chitosan with polylactic acid. Yan et al.[30] reported the grafting of amphiphilic chitosan with PLA matrix to form a film. The obtained film was reported with a uniform dispersion of the chitosan in the PLA matrix. Gupta et al.[31] reported the use of nano amphiphilic chitosan in oligomeric PLA using polymer condensation, which results in better miscibility and thermally stable film than microform of amphiphilic chitosan. Yang et al.[32] and Yanat et al.[33] reported studies on amphiphilic chitosan's use as a compatibilizer between two immiscible polymers. Furthermore, a critical study on the biodegradability and toxicity study of neat amphiphilic chitosan and its blend showed that these properties were not affected by the modification.[28,34,35]

PLA and CNF are having the challenge of agglomeration, which has resulted in low mechanical properties of its composite film. The amphiphilic properties of chitosan were used as a compatibilizer between PLA and CNF in this study.[28,36] In this study, amphiphilic chitosan was prepared and used to enhance polylactic acid's miscibility and properties between PLA and cellulose nanofiber. The CNF was isolated from bamboo using combined alkaline hydrolysis, supercritical carbon dioxide explosion, and high-pressure homogenization. The amphiphilic chitosan was blended with PLA and the isolated CNF as reinforcement. PLA/chitosan/CNF composite was produced using combined melt extrusion and compression molding method.[37] The mechanical, thermal, morphological, and packaging properties of the obtained composite were studied for improved properties.[38] The properties of PLA/chitosan and CNF using this method have not been reported in the literature.

2 | METHODOLOGY

2.1 | Materials

Polylactic acid practical grade (4032D) obtained from Sigma Aldrich, Singapore, was used in this study. The tensile and yield strength of polylactic acid are 62 and 65 MPa, respectively. Its specific gravity and melt extrusion temperature are 1.24, 55–60°C, respectively. Chitin from prawn was deacetylated until 90% and used in this study. The cellulose nanofibrillated fiber used in this study was prepared from *Gigantochloa scortechinii* bamboo. The percentage composition of polylactic acid and chitosan ratio was varied, while CNF was kept constant based on previous studies.[6,39]

2.2 | Composition variation

Based on previous literature on the properties of PLA/CNF, the percentage of cellulose nanofibre was kept constant (5%, Table 1).[22,40] Also, based on previous studies on PLA/chitosan, the composition variation of chitosan is 5%–20% to show the effect on the properties of PLA/chitosan/CNF biocomposite.[40]

2.3 | Preparation and characterization of amphiphilic chitosan

Amphiphilic chitosan was prepared using a substitution reaction of the chitosan heated with excess phthalic anhydride in dried DMF to yield phthayl chitosan (PHCS).[41] It was obtained as a yellow powdery material. The chitosan powder was dissolved in 100 mL of acetic acid. Succinic

anhydride dissolved in methanol was added to the chitosan solution and heated at 50°C for 8 h with stirring. The resulting colloid mixture was precipitated with $NaHCO_3$ with stirring for 1 h[28] to form a semi-solid gel. The resulting semi-solid gel was washed with distilled water until neutral pH. The gel precipitate was freeze-dried and ground into powder. The amphiphilic chitosan powder was stored in a zip lock bag for testing and biocomposite preparation. The FT-IR functional group analysis of the chitosan and amphiphilic chitosan was conducted with FT-IR (EFTEM Libra—Carl Zeiss, UK), to study the successful modification process.

2.4 | Isolation and characterization of Cellulose nanofibrillated fiber

CNF was prepared using the method reported by Atiqah et al.[6] with modification. The cellulose nanofibrillated fiber was prepared using combined alkaline hydrolysis, supercritical SC-CO_2 explosion, and high-pressure homogenization. The CNF was prepared from oven-dried Gigancolar (*G. scortechinii*) bamboo fiber. The bamboo fiber was heated for 4 h in a sodium hydroxide (25%) and anthraquinone (0.2%) at a temperature of 160°C to form a pulp. The extractives and degraded hemicellulose were removed by washing with distilled water. This was followed by 2 h bleaching process of the pulp with sodium hydroxide (3%, NaOH), hydrogen peroxide (3%, H_2O_2), and magnesium sulphate (0.5%, $MgSO_4$) at 80°C. The bleached fibers were washed with water till neutral pH was obtained and subjected to 2 h supercritical carbon dioxide (SC-CO_2) 50 MPa explosion at 60°C to obtain CNFs. The obtained CN was finally subjected to high-pressure homogenization to further reduce the fiber sizes.

The CNF produced was analyzed with FT-IR and transmission electron microscopy (TEM). The FT-IR samples were prepared with potassium bromide (KBr) from a thin film and placed in an FT-IR machine to obtain the functional group bands for the wavenumber. The TEM CNF samples were prepared in water, and droplet stains were placed on the copper led. The droplet was stained with acetone and observed under TEM (Perkin-Elmer, PC1600, Winter Street Waltham, MA, USA) at 100 nm and 40 kV potential. The CNF zeta potential for stability was analyzed with Zetasizer Ver. 6.11, (Malvern, UK). The CNF aqueous suspension was prepared using 0.01 mg in 5 mL of distilled water of refractive index 1.330 and sonicated for 10 min.[6] The zeta potential was obtained in 0.1 mM KCl electrolyte using the machine.

TABLE 1 Composition variation

Sample name	Polylactic acid (wt%)	Chitosan (wt%)	CNF (wt%)
P80205	80	20	5
P85155	85	15	5
P90105	90	10	5
P9555	95	5	5
P1005	100	0	5
PLA	100	0	0

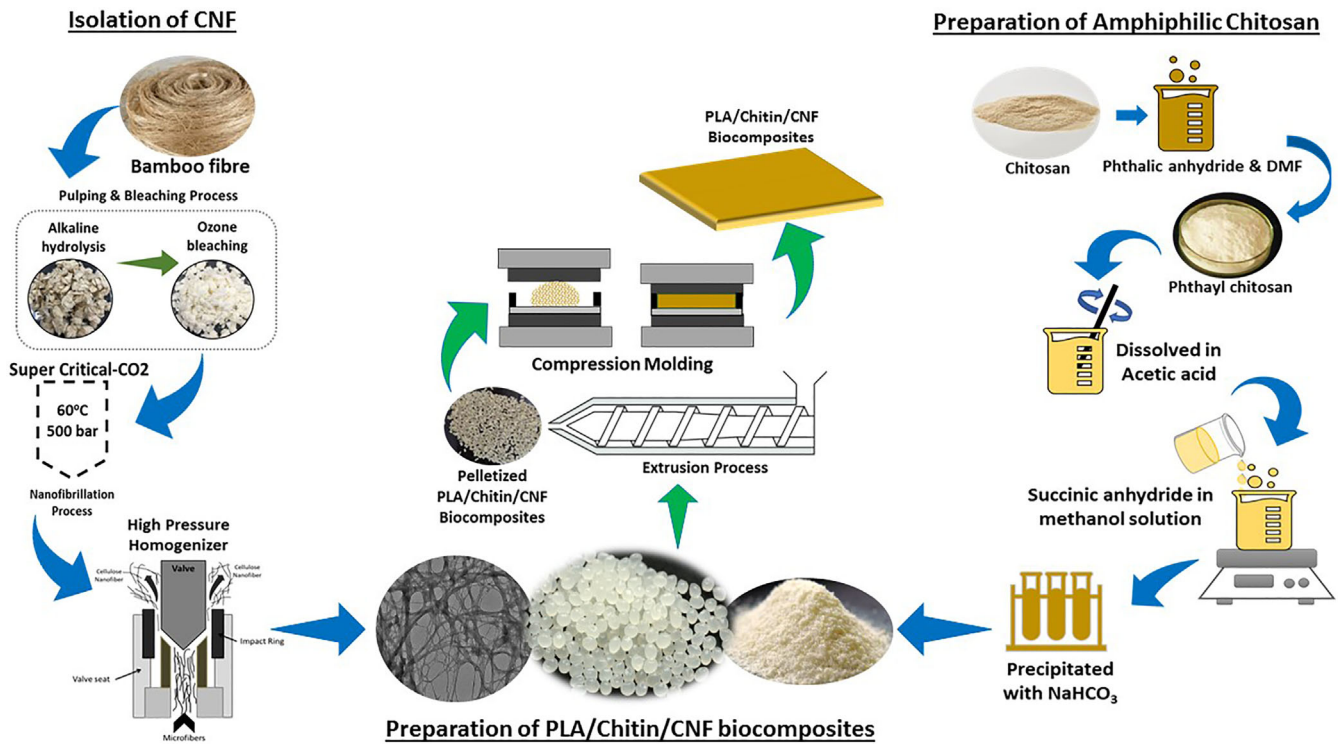

SCHEME 1 Preparation of amphipilic chitosan, isolation of cellulose nanofiber, and preparation of PLA/chitosan/CNF biocomposite

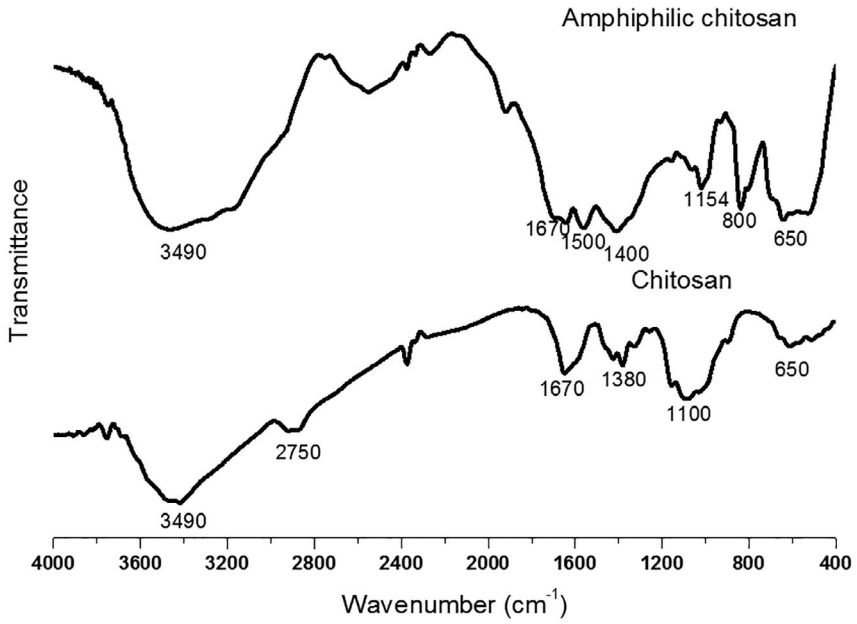

FIGURE 1 FT-IR graph of amphiphilic chitosan and conventional chitosan

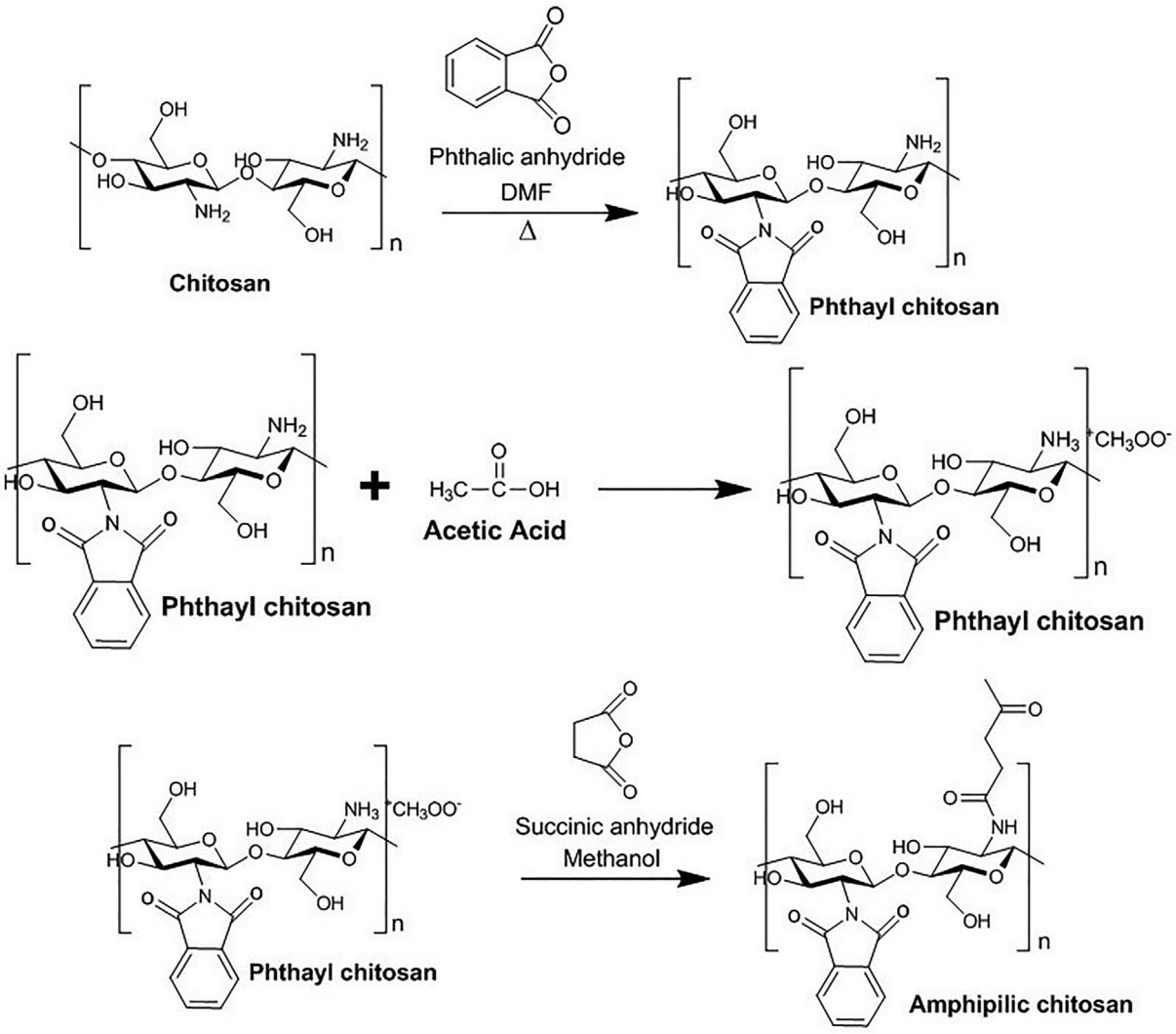

SCHEME 2 Preparation and chemical reaction of amphiphilic chitosan

2.5 | Preparation of PLA/chitosan/CNF biocomposite

The PLA/chitosan/CNF biocomposite was prepared with combined melt extrusion and compression molding technique (Scheme 1). The freeze-dried amphiphilic chitosan, CNF, and PLA were thoroughly mixed with a rheometer and extruded with a twin-screw extruder at 100 kg/min, a temperature profile range of 120–180°C from filament. The filament was pelletized with a pelletizer at a rate of 30 rpm. The pelletized biocomposite was compressed with a carver press compression molding machine to rectangular boards at a temperature of 150°C and a pressure of 5 MPa. The rectangular board was cut into test samples using a milling cutter and stored in a zip lock bag. The schematic diagram of the amphiphilic chitosan preparation process, cellulose nanofiber, and biocomposite is shown in Scheme 1.

2.6 | Characterization of PLA/chitosan/CNF biocomposite

The tensile properties of the neat PLA and PLA/chitosan/CNF biocomposite were measured with (MT1175 Dia-Stron Instruments, Andover, UK), using ASTM D3039 as standard. Five replicates of dumbbell-shaped samples with standard sizes were molded and tested to obtain the tensile strength, elongation, and tensile modulus. The tensile fractured surface morphological properties of the biocomposite were observed with scanning electron microscopy (SEM). The SEM samples were prepared from the tensile samples' fractured surface and coated with carbon to enhance its conductivity for observation under the scanning machine. The coated samples were observed with SEM (EVO MA 10, Carl-ZEISS SMT, Oberkochen, Germany), to obtain the 1000 magnification images of each sample at 200 μm and 40 kV.

The structural properties of the biocomposite were studied with X-ray diffraction and FT-IR analysis. The X-ray diffraction (XRD) micrograph was conducted with the powder form of the neat PLA. PLA/chitosan/CNF biocomposite using a X-ray diffractometer (PANalytical X'Pert PRO X-ray Diffraction) at a diffraction angle range of $2\theta = 10°–50°$, 1.540598 for K-alpha 1 and K-alpha 2 wavelength, 45 V, and a tube current of 40 A. FT-IR analysis of the biocomposite was conducted using its powder form. The sample powder was mixed with potassium bromide (KBr) and pressed into the circular film. The circular film was placed in the FT-IR machine, and the absorption band of the functional groups was obtained.

The thermogravimetry analysis (TGA) and derivative thermogravimetry analysis (DTA) of the neat PLA, PLA/CNF, and the PLA/chitosan/CNF biocomposite samples were studied at a temperature range of 40–800°C and 20°C/min temperature change. A mass range of 5–10 mg of the neat PLA, PLA/CNF, and biocomposites was used as the TGA-DTA samples. The percentage rate of degradation (weight decrease) of the biocomposite with temperature was recorded and analyzed. The differential scanning calorimetry of neat PLA biocomposites was obtained using a DSC analyzer to study the melting and crystallization peaks. The obtained data were analyzed with a

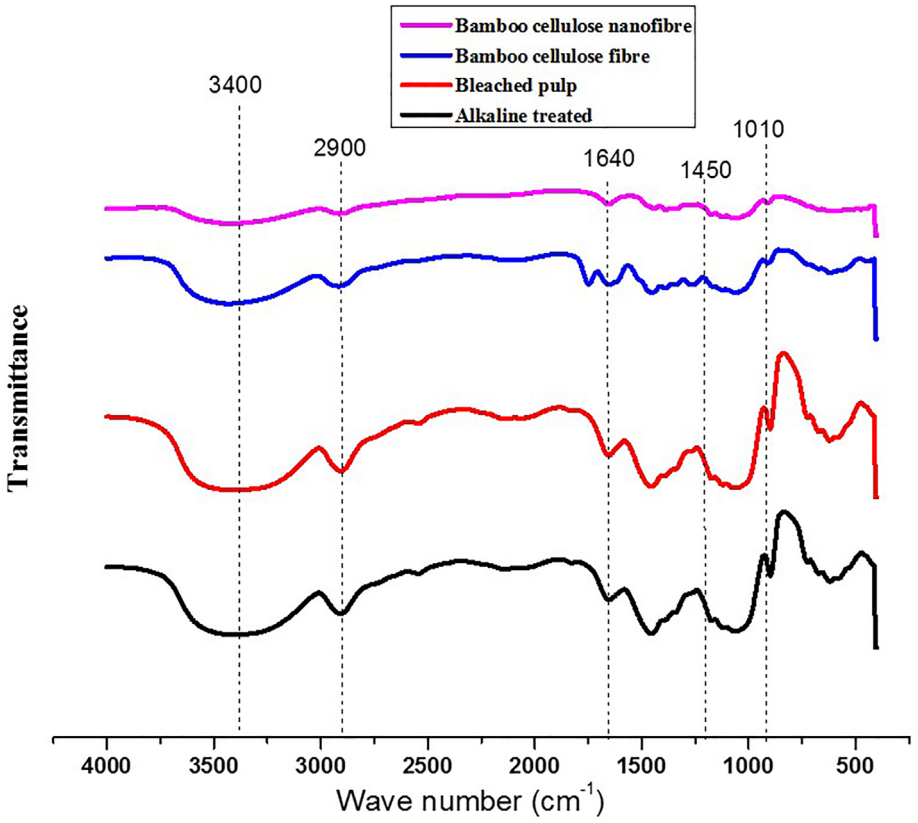

FIGURE 2 FT-IR analysis of bamboo fiber and cellulose nanofibre during the isolation process

DSC software and plotted with origin software. Powdered samples of the neat PLA and biocomposite with a mass range between 5 and 10 mg were used for the test. DSC analysis was done at a temperature range of 50–200°C at a rate of 20°C/min.

The biopolymers' wettability properties were measured with water absorption, the thickness of swelling, and contact angle. The water absorption properties of the neat PLA and PLA/chitosan/CNF biocomposite were calculated from Equation (1). The samples were cut to sizes 2 × 2 cm with a cutter machine and oven-dried for 72 h. The samples were preweighed (w_1) and immersed in water for 24 h based on ASTM D570. The samples were removed and surface dried before the final weight (w_2) of the samples was taken, and the water absorption was calculated with Equation (1)

$$\text{Water absorption}\,(\%) = \frac{w_2 - w_1}{w_1} \times 100 \quad (1)$$

The initial thickness (t_1) and final thickness (t_2) of the neat PLA and the biocomposite samples were also documented. The value of the thickness of swelling was obtained using Equation (2)

$$\text{Thickness of swelling}\,(\%) = \frac{t_2 - t_1}{t_1} \times 100 \quad (2)$$

Furthermore, the contact angle of neat PLA and PLA/chitosan/CNF biocomposite was measured. The samples' contact angle was measured with a contact angle analyzer (KSV CAM 101; KSV Instruments Ltd., Helsinki, Finland. Five replicates of the samples were used for the measurement, and the average values were calculated.

3 | RESULT AND DISCUSSION

3.1 | Properties of amphiphilic chitosan

The results of the FT-IR analysis of chitosan and modified chitosan are presented in Figure 1(A). The result showed a band between 3100 and 3500 cm^{-1} for both unmodified and modified chitosan, representing OH and NH stretching. A small peak was observed between 2800 and 2930 cm^{-1} representing aldehyde —C—H stretches on the unmodified chitosan. Also, a short peak at 1600–1680 cm^{-1} is termed C═O stretching from the amide functional group and acetylation of the amino group. The 1550 (CO_2^-), 1400 band sp3 —C—H bend, 1154 C—O—C bridge, 800 and 650 cm^{-1} are alkene sp^2 C—H bending. The presence of the 800 band in the modified chitosan showed the presence of alkene C—H bending, and the increase in the 650 bands showed the presence of C—H bond indicating alkyl group. The changes or emergence of new peaks bands 1500 and 800 cm^{-1} are a typical indication of alkyl group attachment (substitution) to the chitosan chain. Previous studies on this modification process reported that the alkyl group attachment occurred at the amine functional group present in the chitosan.[28,41] The hydrogen atoms of -NH_2 were substituted for during the modification. The chemical reaction equation for the modification process is presented in Scheme 2.

3.2 | Properties of isolated cellulose nanofibrillated fiber

The FT-IR spectrum of isolated CNF from bamboo using combined supercritical and high-pressure homogenization is shown in Figure 2. The FT-IR analysis result showed three main regions of bands. The transmittance band of -OH stretches between 3300 and 3600 cm^{-1}, symmetric and antisymmetric vibration of CH_2 between 2819 and 2900 cm^{-1},[42] and the bond at 1610 cm^{-1} to 1648 can be attributed to OH bending of adsorbed water.[42] These bands have been reported

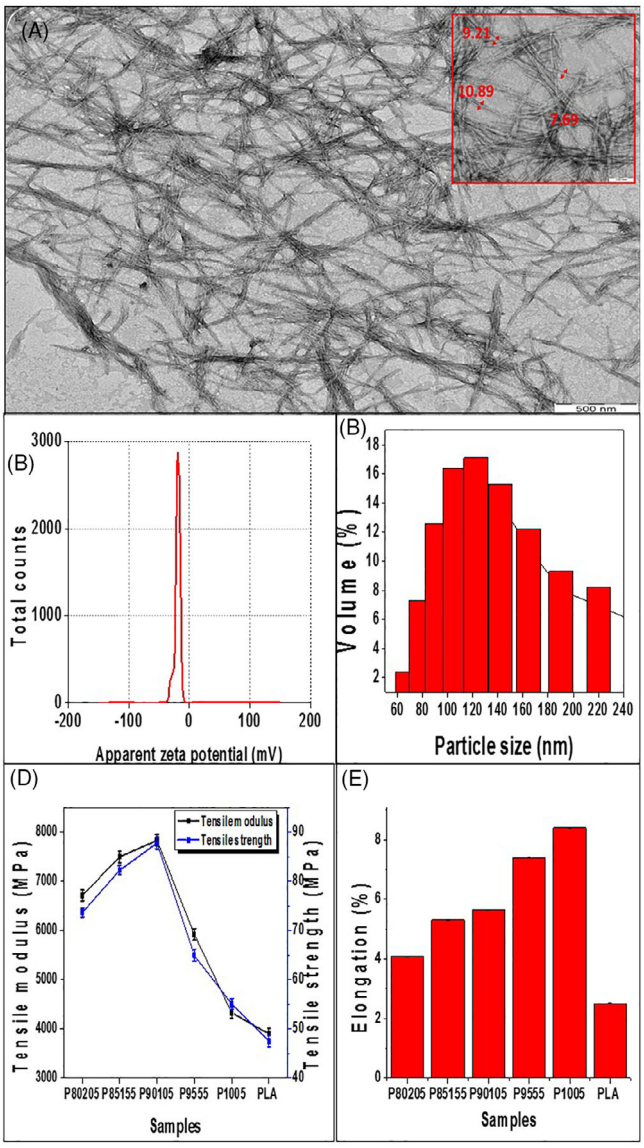

FIGURE 3 (A) Transmission electron microscope, (B) zeta potential, and (C) particle size analyses of isolated bamboo cellulose nanofiber, (D) tensile strength and modulus, and (E) elongation of PLA/chitosan/CNF biopolymer composite

in the previous literature on the isolation of cellulose nanofiber.[6,22] The bands between 1500 and 1700 cm^{-1} are probably due to the presence of hemicellulose and lignin. These peaks were observed to disappear with the isolation of cellulose nanofiber. These showed that the isolation process effectively removed these components' purity.[43,44] Other peak ranges are 1410–1420 cm^{-1} for CH_2 scissoring motion, 1368–1373 cm^{-1} for CH bending, ~1317 cm^{-1} for CH_2 wagging42 and the bands between 1000 and 1250 cm^{-1} can be associated with C—O—C stretching (glycosidic linkage) present in cellulose.[45,46] These are basic typical bonds present in cellulose or nanocellulose, and the only difference between the FT-IR graphs is the transmittance percentage. Furthermore, it was observed that no new bond was obtained from the isolation process, which is an indication that the chemicals have no chemical bonding with the bamboo fibers. This is very significant to the isolation process because any emerging new bands meant alteration of the original cellulose structure and emergence of new properties.[46]

The result of transmission electron microscopy, particle sizes analysis, and zeta potential of isolated CNF are shown in Figure 3(A)–(C). TEM images confirmed the effectiveness of combining supercritical CO_2 and high-pressure homogenization methods in cellulose nanofiber isolation. The images showed a network of fiber with spaghetti-shaped strands. The diameters of the fibers measured in the TEM image (shown with the red arrows in Figure 3(A)) confirmed cellulose nanofibers' formation. The zeta potential is crucial to the nanofiber's stability in a colloidal system (aggregation and sedimentation). Generally, a high zeta potential value, either positive or negative, showed good stability of the nanoparticle suspension, which means

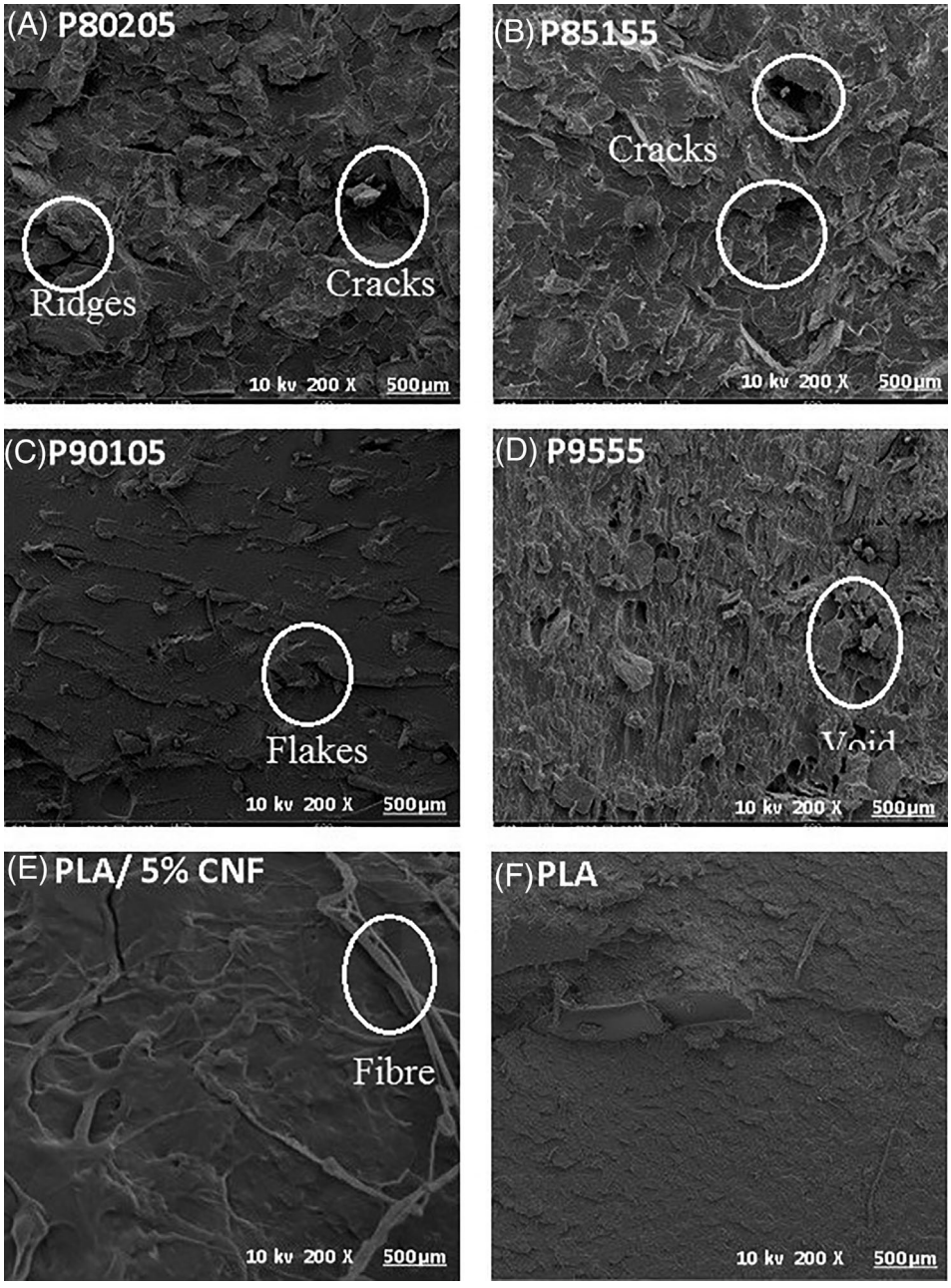

FIGURE 4 Morphological properties (SEM) of PLA/chitosan/CNF biopolymer composite; (A) P80205, (B) P85155, (C) P90105, (D) P9555, (E) PLA/CNF (P1005), and (F) neat PLA

that the repulsion forces exceed that of the attractive forces. The zeta potential value of isolated cellulose nanofiber showed a potential value of −50 mV, which is quite high. This means that the obtained cellulose nanofiber is stable, and no reversal of the process even if it is in suspension. Similar potential values for cellulose nanofiber as reported in previous literature[47,48] Furthermore, the result obtained from particle size analysis shows nano sizes. The fiber diameter varies between 60 nm and 220 nm, with peak particle size at 12 nm (Figure 3(C)). This fiber size range is considered nano and has been reported in previous studies on CNF isolation.[8,49]

3.3 | Properties of isolated cellulose nanofibrillated fiber and PLA/chitosan/CNF biocomposite

The results of tensile properties of the PLA/chitosan/CNF biocomposites (P80205, P85155, P90105 P9555), PLA/CNF (P1005), and neat PLA are presented in Figure 3(D), (E). The tensile strength and modulus values (Figure 3(D))) were observed to increase with amphiphilic chitosan's addition until 10% and, after that, a drop in the value. However, the tensile strength and modulus values were generally higher than those of the neat PLA and PLA/CNF, which serve as the control. This trend in the observed tensile strength and modulus is expected, as reported in the previous studies on fillers and reinforcement on the PLA matrix.[22,48] The increase in strength is associated with forming a chemical bonds or interfacial interactions between the matrix and the reinforcement. Generally, the elongation values of the PLA/chitosan/CNF and PLA/CNF were higher than those of the neat PLA. The elongation of PLA/chitosan/CNF biocomposite (Figure 3(E)) was observed to decrease with an increase in the percentage of amphiphilic chitosan. However, the elongation value of PLA/CNF was significantly higher than that of the PLA/chitosan/CNF biocomposites. The observed trend is probably due to the enhanced stiffness of the biocomposite with the addition of chitosan fillers.[26,39]

The results of the tensile fractured surface of PLA/chitosan/CNF biocomposites (P80205, P85155, P90105 P9555), PLA/CNF (P1005), and neat PLA are presented in Figure 4. The fractured surface was studied to observe the miscibility enhancement of amphiphilic chitosan. It showed a well-compacted homogenous surface for the biocomposite as observed for P80205, P85155, P90105, and P9555 with minor voids and had uniform coloration with no segregation. On the other hand, the SEM image of PLA/CNF showed fiber-like strands on the fractured surface due to the presence of CNF not thoroughly mixed with the PLA matrix. These fiber strands are seen to dominate the fractured surface of PLA/CNF, with the matrix appearing to be below the strands. Compared with the neat PLA, the SEM of PLA/CNF and PLA/chitosan/CNF is rough with wedge-like ridges. The ridges are probably due to the presence of filler (chitosan) or reinforcement (CNF), or both, as the case may be. The sharpness in the wedges of the PLA/chitosan/CNF may indicate brittleness with an increase in modified chitosan percentage. A review of the previous studies on PLA/CNF composite reported similar fiber and matrix separation (segregation).[6,22] Several modification techniques have been adapted to solve the challenge of immiscibility between PLA and CNF due to their nature.[22,24,50] The use of amphiphilic chitosan as a bridge between hydrophilic CNF and hydrophobic PLA could be a permanent solution. In this study, the fiber and matrix separation were observed (Figure 4(A)–(C)) to disappear with the incorporation of amphiphilic chitosan, resulting in enhanced miscibility.

The FT-IR spectra of the neat PLA, PLA/CNF (P1005), and PLA/chitosan/CNF biocomposite (P80205, P85155, P90105, P9555) are presented in Figure 5. The FT-IR studies of the biocomposite were compared with the neat PLA. Similar bands in the precursor materials (PLA, chitosan, and CNF) were observed in the biocomposite spectra.[40] However, the absorbance for each of the bands was reduced in intensity. The FT-IR spectra between 3400 and 3650 cm^{-1} are due to

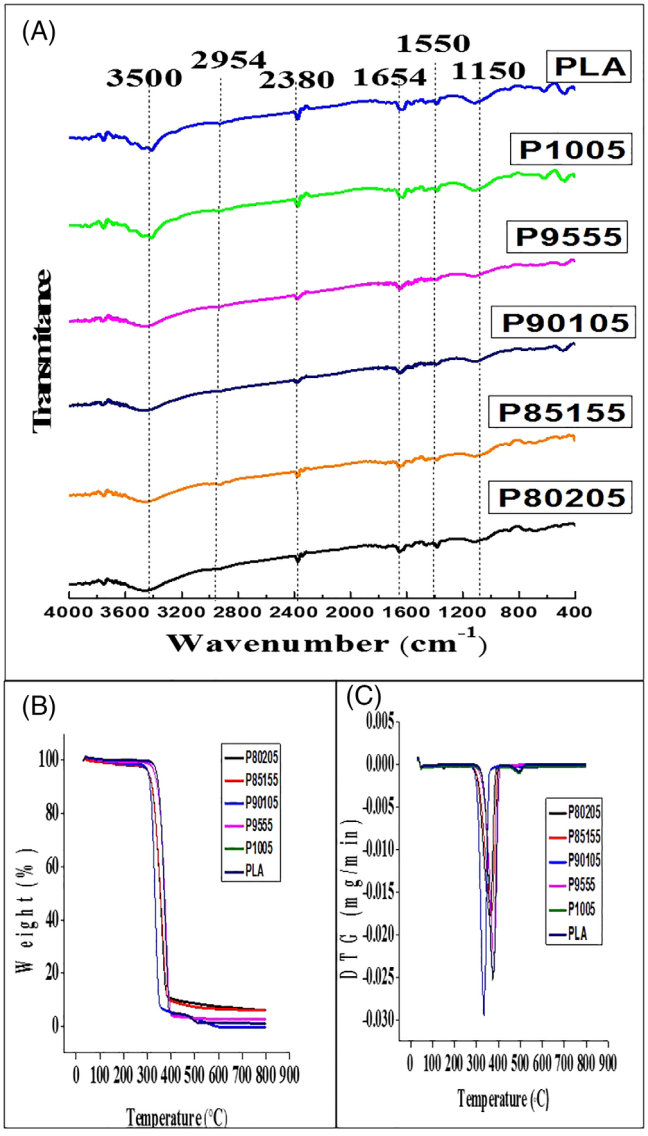

FIGURE 5 FIGURE(A) FT-IR analysis, (B) thermogravimetry analysis (TGA), and (C) derivative thermogravimetry analysis of PLA/chitosan/CNF biopolymer composite

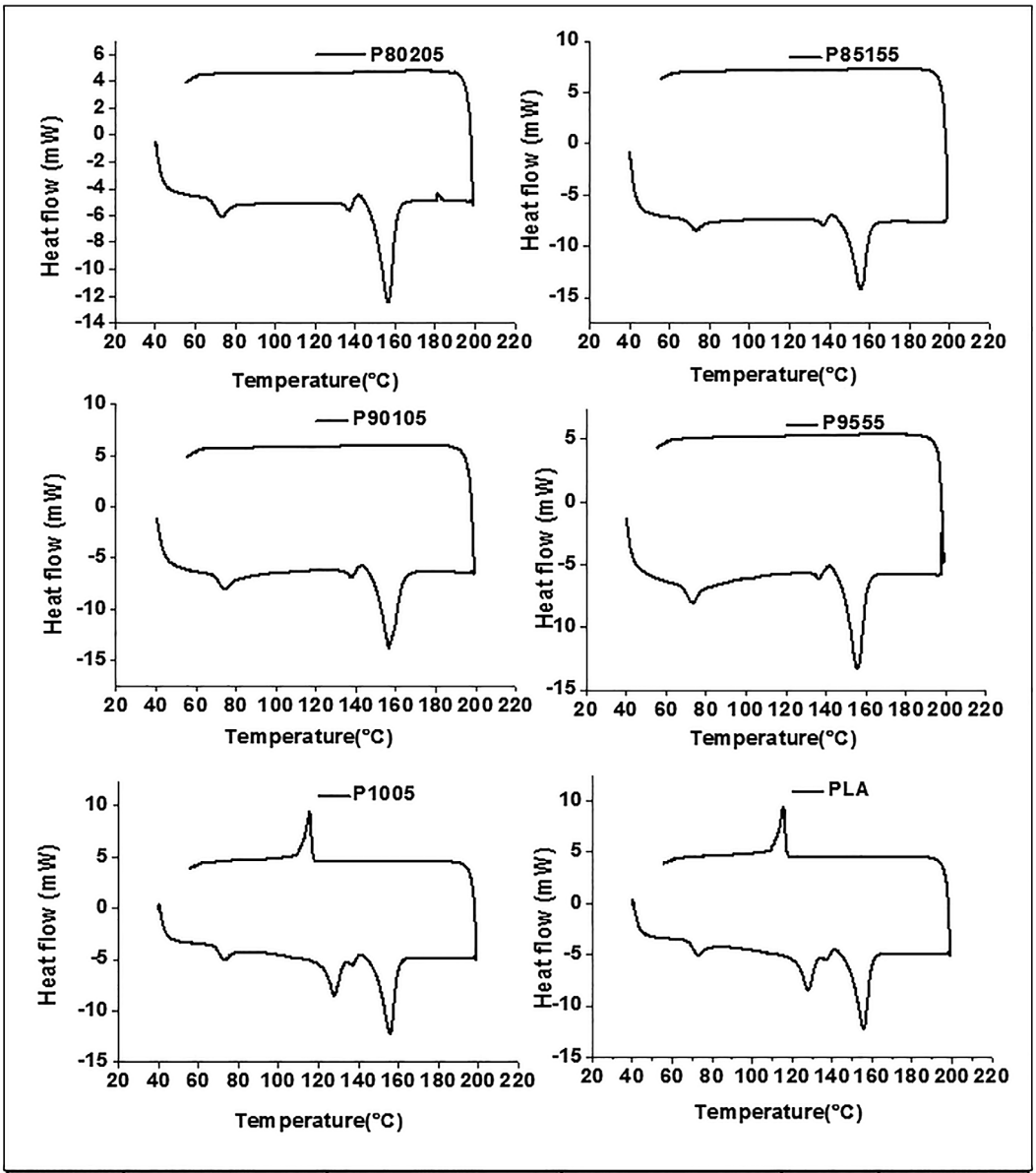

P80205	9.26	73.27	-	-	156.55
P85155	5.65	73.22	-	-	156.42
P90105	5.77	74.13	-	-	156.33
P9555	6.25	73.27	-	-	155.61
P1005	6.01	72.92	118.30	128.68	155.50
PLA	6.71	72.86	117.45	128.50	155.83

FIGURE 6 FIGUREDifferential scanning calorimetry (DSC) properties of PLA/chitosan/CNF biocomposites; (A) P80205, (B) P85155, (C) P90105, (D) P9555, (E) PLA/CNF (P1005), and (F) neat PLA

the —OH band present in chitosan and CNF. The band at 2950 cm^{-1} assigned to —C—H stretching vibrations is typically present in PLA, chitosan, and CNF. The spectra band at 1654, 1599, and 1550 cm^{-1} are assigned to amide like those present in chitosan. However, some previously observed peaks such as 1154, 850, and 650 cm^{-1} in the modified chitosan were not observed in the biocomposite. In general, no significant new bond was formed between the precursor materials.[39] This means major interactions between the precursor materials will be interfacial based on their nature (hydrophilic or hydrophobic). This shows that the morphological studies' good miscibility is essentially due to the chitosan's natural modification, which serves as a bridge between the two materials.[26]

The results of the thermogravimetry analysis (TGA) of the neat PLA, PLA/CNF, and PLA/chitosan/CNF biocomposite are shown in Figure 5(B)). The graph displays the weight loss in percentage to the temperature change, which is a measurement of the composite's stability to heating. The TGA curve showed a single degradation curve for both the neat PLA and the biocomposites. The single curve degradation is probably a significant pointer to the good miscibility of the three polymers. The onset temperature for P80205, P85155, P90105, P9555, P1005, and neat PLA are 260, 263, 267, 271, 273, and 275°C, respectively. The onset temperature values indicated that chitosan's addition enhanced the early start of the degradation process compared with the neat PLA. Furthermore, the DTG curve (Figure 5(C))) peak temperature values for P80205, P85155, P90105, P9555, P1005, and neat PLA are 350, 357, 340, 370, 373, and 375 °C, respectively. It was observed from these values that the addition of chitosan also reduced the DTG peak temperature, which showed that it enhances the thermal degradation properties of the biocomposite. The percentage weight loss for P80205, P85155, P90105, P9555, P1005, and neat PLA are 93.3%, 94.0%, 96.3%, 97.3%, 98.1%, and 98.9%, respectively. The percentage weight loss values showed an increase in carbon deposit after the biocomposite's thermal degradation with an increased percentage of chitosan as expected.[26,51]

The differential scanning calorimetry result is shown in Figure 6 for neat PLA and biocomposite. In the figure, T_g represents the glass transition temperature, T_c is crystallinity temperature, and T_m is the melting temperature. The values of T_g, T_c, and T_m are presented in tabular form (Figure 6). The T_g for the neat PLA, PLA/CNF, and PLA/the biocomposite was observed to peak at P90105. The T_g values are seen to increase with the addition of CNF and chitosan. The T_c values were only observed for neat PLA and PLA/CNF in the cooling curve. The T_m values for P1005, and P9555 biocomposites are lower compared to that of neat PLA. However, the T_m for P90105, P85155, and P80205 biocomposite is higher than that of neat PLA. Generally, for the PLA/chitosan/CNF biocomposites, the T_m is observed to increase with the addition of chitosan. This result corroborated the DTG result, which showed a shift in its peak with chitosan addition. A similar result on the effect of the addition of chitosan and CNF on the thermal properties of PLA has been reported in the previous studies on PLA/chitosan and PLA/CNF[40] biocomposites.[26,52] The thermal properties' changes have been attributed to the interaction (physical or chemical) between the PLA matrix and the reinforcement. These interactions could be chemical or physical (adhesion and cohesion forces); however, a specific chemical bonding between the three polymers has not been reported.

The thickness of the swelling, contact angle, and water absorption properties of the neat PLA, PLA/CNF, and PLA/chitosan/CNF biocomposite are shown in Figure 7. The thickness of swelling measured with a micrometer screw gauge for each sample showed increased value, with the neat PLA having the lowest and P80205 as the highest. The contact angle (CA) measurements of neat PLA, PLA/CNF, and PLA/chitosan/CNF biocomposite were conducted to study the effects of chitosan and CNF on PLA's hydrophobicity. The result of the contact angle is shown in Figure 7. The neat PLA has the highest contact angle measurement, a typical representation of its hydrophobic nature. However, the contact angle value was observed to significantly reduce with the addition of both chitosan and CNF. The neat PLA has a contact angle value of 87° and the contact value reduced to 79°, 75°, 73°, 69°, and 65° for P1005, P9555, P90105, P85155,

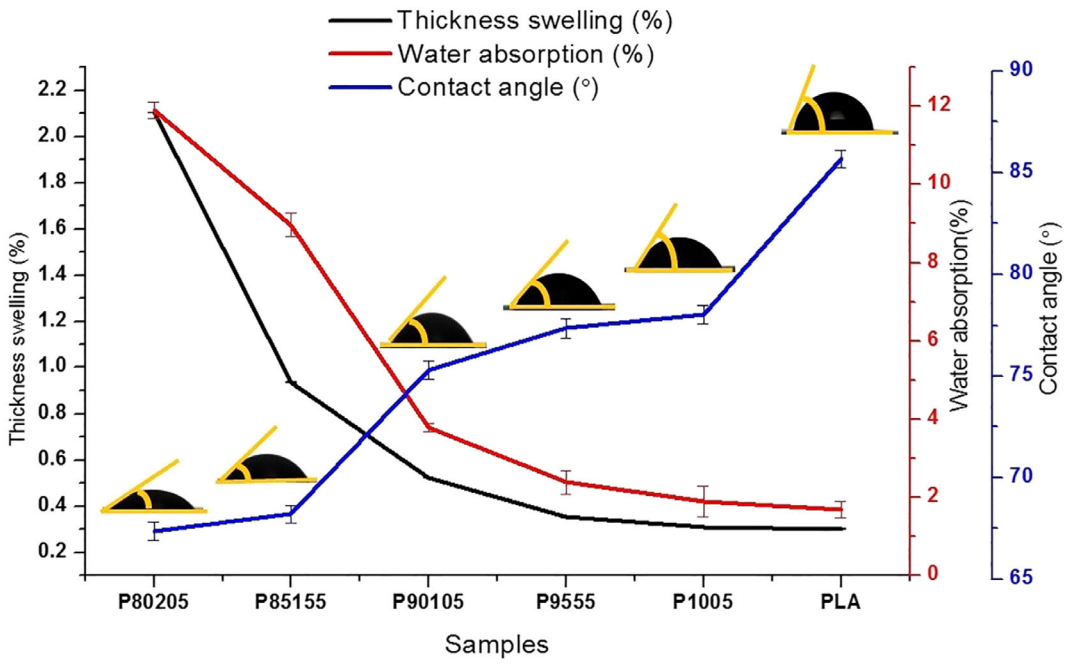

FIGURE 7 Wettability properties of PLA/chitosan/CNF biopolymer composite (A) P80205, (B) P85155, (C) P90105, (D) P9555, (E) PLA/CNF (P1005), and (F) neat PLA]

and P80205, respectively. The reduction of the contact angle value is still indicated that the PLA films are still hydrophobic. The contact angle values showed that the biocomposite has a new wettability property different from neat PLA. The water absorption of the neat PLA, PLA/CNF, and PLA/chitosan/CNF was plotted alongside the contact angle to validate the result. The water absorption result showed an increasing trend with the addition of CNF and chitosan. The neat PLA had the lowest water uptake after 24 h while P80205 has the highest. The increase in water absorption properties can be attributed to the hydroxyl-containing functional group in the structure of chitosan and CNF.[40,53] The hydroxyl (—OH) functional group of the CNF is responsible for the increased water uptake in PLA/CNF biocomposite.[40] Chitosan also significantly affects water absorption because it possesses a hydroxy-functional group apart from the amine functional group.[26,39] The presence of a hydroxy group in the biocomposite increased hydrogen bonding formation with water molecules.[54]

4 | CONCLUSION

The isolation of CNF was successfully done using combined chlorine-free bleaching, supercritical carbon dioxide, and high-pressure homogenization. Also, the amphiphilic chitosan was successfully prepared in this study, and PLA/chitosan/CNF biocomposite was produced with no agglomeration. The effect of amphiphilic chitosan on PLA/CNF biopolymer composite properties was studied and discussed. The miscibility and mechanical properties of PLA/CNF were successfully enhanced with amphiphilic chitosan. The result showed significant improvement in mechanical, thermal, and wettability properties. The properties' significant improvement was due to the compatibilizer effect of amphiphilic chitosan PLA/chitosan/CNF biocomposite. The PLA/chitosan/CNF biocomposite result showed its potential used as packaging material for nonfood products.

ACKNOWLEDGMENTS

The authors would like to acknowledge and express their gratitude towards the collaboration between Universitas Sumatera Utara, Indonesia, Universiti Pendidikan Sultan Idris, Indonesia, and Universiti Sains Malaysia, Penang, Malaysia that has made this work possible.

This work was financially supported by the Ministry of Educan, RUI/1001/PTEKIND8014119.

DATA AVAILABILITY STATEMENT

The data that support the findings of this study are available from the corresponding author upon reasonable request.

ORCID

Abdul Khalil H. P. S. https://orcid.org/0000-0003-2403-809X

REFERENCES

1. Sanusi OM, Benelfellah A, Bikiaris DN, Aït HN. Effect of rigid nanoparticles and preparation techniques on the performances of poly (lactic acid) nanocomposites: a review. *Polym Adv Technol*. 2020; 12(2):444-460.
2. Uthaya Kumar US, Abdulmadjid S, Olaiya N, et al. Extracted compounds from neem leaves as antimicrobial agent on the Physicochemical properties of seaweed-based biopolymer films. *Polymer*. 2020;12(5):1119.
3. Zhang Y, Jia S, Pan H, et al. Preparation, characterization and properties of biodegradable poly (butylene adipate-co-butylene terephthalate)/thermoplastic poly (propylene carbonate) polyurethane blend films. *Polym Adv Technol*. 2020;32(2):613-629.
4. Saba N, Jawaid M, Alothman OY, Paridah M, Hassan A. Recent advances in epoxy resin, natural fiber-reinforced epoxy composites and their applications. *J Reinf Plast Compos*. 2016;35(6):447-470.
5. Khan T, Hameed Sultan MTB, Ariffin AH. The challenges of natural fiber in manufacturing, material selection, and technology application: a review. *J Reinf Plast Compos*. 2018;37(11):770-779.
6. Atiqah M, Gopakumar DA, FAT O, et al. Extraction of cellulose nanofibers via eco-friendly supercritical carbon dioxide treatment followed by mild acid hydrolysis and the fabrication of cellulose nanopapers. *Polymer*. 2019;11(11):1813.
7. Kumar KP, Sekaran ASJ. Some natural fibers used in polymer composites and their extraction processes: a review. *J Reinf Plast Compos*. 2014;33(20):1879-1892.
8. Abdul Khalil HPS, Adnan A, Yahya EB, et al. A review on plant cellulose nanofibre-based aerogels for biomedical applications. *Polymer*. 2020;12(8):1759.
9. Rizal S, Abdullah CK, Olaiya NG, et al. Preparation of palm oil ash nanoparticles: Taguchi optimization method by particle size distribution and morphological studies. *Appl Sci*. 2020;10(3):985.
10. Ahmed J, Varshney SK. Polylactides—chemistry, properties and green packaging technology: a review. *Int J Food Prop*. 2011;14(1):37-58.
11. Muthuraj R, Misra M, Mohanty AK. Biodegradable compatibilized polymer blends for packaging applications: a literature review. *J Appl Polym Sci*. 2018;135(24):45726.
12. Brebu M. Environmental degradation of plastic composites with natural fillers—a review. *Polymer*. 2020;12(1):166.
13. García-Campo MJ, Boronat T, Quiles-Carrillo L, Balart R, Montanes N. Manufacturing and characterization of toughened poly (lactic acid) (PLA) formulations by ternary blends with biopolyesters. *Polymer*. 2018;10(1):3.
14. Olaiya NG, Nuryawan A, Oke PK, et al. The role of two-step blending in the properties of starch/chitosan/polylactic acid biodegradable composites for biomedical applications. *Polymer*. 2020;12 (3):592.
15. Rajesh G, Prasad AR, Gupta A. Mechanical and degradation properties of successive alkali treated completely biodegradable sisal fiber reinforced poly lactic acid composites. *J Reinf Plast Compos*. 2015;34 (12):951-961.
16. Zeng J-B, Li K-A, Du A-K. Compatibilization strategies in poly(lactic acid)-based blends. *RSC Adv*. 2015;5(41):32546-32565.
17. Nejati S, Karimi-Soflou R, Karkhaneh A. Influence of process parameters on the characteristics of oxygen-releasing poly (lactic acid) microparticles: a multioptimization strategy. *Polym Adv Technol*. 2020;32(2): 829-841.
18. Riaz S, Fatima N, Rasheed A, Riaz M, Anwar F, Khatoon Y. Metabolic engineered biocatalyst: a solution for PLA based problems. *Int J Biomater*. 2018;2018:1-9.
19. Siakeng R, Jawaid M, Ariffin H, Sapuan S, Asim M, Saba N. Natural fiber reinforced polylactic acid composites: a review. *Polym Compos*. 2019;40(2):446-463.
20. Gupta B, Revagade N, Hilborn J. Poly (lactic acid) fiber: an overview. *Prog Polym Sci*. 2007;32(4):455-482.
21. Pang X, Zhuang X, Tang Z, Chen X. Polylactic acid (PLA): research, development and industrialization. *Biotechnol J*. 2010;5(11): 1125-1136.

22. Clarkson CM, El Awad Azrak SM, Chowdhury R, et al. Melt spinning of cellulose nanofibril/polylactic acid (CNF/PLA) composite fibers for high stiffness. *ACS Appl Polym Mater*. 2018;1(2):160-168.
23. Wang Q, Ji C, Sun J, Zhu Q, Liu J. Structure and properties of Polylactic acid biocomposite films reinforced with cellulose Nanofibrils. *Molecules*. 2020;25(14):3306.
24. Zhang Q, Lei H, Cai H, et al. Improvement on the properties of microcrystalline cellulose/polylactic acid composites by using activated biochar. *J Clean Prod*. 2020;252:119898.
25. Wijesena RN, Tissera ND, Abeyratne C, et al. In-situ formation of supramolecular aggregates between chitosan nanofibers and silver nanoparticles. *Carbohydr Polym*. 2017;173:295-304.
26. Hassan MM, Koyama K. Thermomechanical and viscoelastic properties of green composites of PLA using chitosan micro-particles as fillers. *J Polym Res*. 2020;27(2):27.
27. Philippova O, Korchagina E. Chitosan and its hydrophobic derivatives: preparation and aggregation in dilute aqueous solutions. *Polym Sci Ser A*. 2012;54(7):552-572.
28. da Mata CO, Lima AMF, Assis OBG, Tiera MJ, de Oliveira Tiera VA. Amphiphilic diethylaminoethyl chitosan of high molecular weight as an edible film. *Int J Biol Macromol*. 2020;164:3411-3420.
29. Zamboulis A, Nanaki S, Michailidou G, et al. Chitosan and its derivatives for ocular delivery formulations: recent advances and developments. *Polymer*. 2020;12(7):1519.
30. Wu Y, Zheng Y, Yang W, Wang C, Hu J, Fu S. Synthesis and characterization of a novel amphiphilic chitosan–polylactide graft copolymer. *Carbohydr Polym*. 2005;59(2):165-171.
31. Gupta A, Pal AK, Woo EM, Katiyar V. Effects of amphiphilic chitosan on Stereocomplexation and properties of poly (lactic acid) Nano-biocomposite. *Sci Rep*. 2018;8(1):1-13.
32. Yang M-C, Tseng Y-Q, Liu K-H, et al. Preparation of amphiphilic chitosan–graphene oxide–cellulose nanocrystalline composite hydrogels and their biocompatibility and antibacterial properties. *Appl Sci*. 2019;9(15):3051.
33. Yanat M, Schroën K. Preparation methods and applications of chitosan nanoparticles; with an outlook toward reinforcement of biodegradable packaging. *React Funct Polym*. 2021;104849:1-12.
34. Yu H, Wang W, Chen X, Deng C, Jing X. Synthesis and characterization of the biodegradable polycaprolactone-graft-chitosan amphiphilic copolymers. *Biopolymers*. 2006;83(3):233-242.
35. Feng H, Dong C-M. Preparation, characterization, and self-assembled properties of biodegradable chitosan– poly (l-lactide) hybrid amphiphiles. *Biomacromolecules*. 2006;7(11):3069-3075.
36. Antipova CG, Lukanina KI, Krasheninnikov SV, et al. Study of highly porous poly-l-lactide-based composites with chitosan and collagen. *Polym Adv Technol*. 2020;32(2):853-860.
37. Tham MW, Fazita MN, Abdul Khalil HPS, et al. Tensile properties prediction of natural fibre composites using rule of mixtures: a review. *J Reinf Plast Compos*. 2019;38(5):211-248.
38. Lopes AC, Barcia MK, Veiga TB, Yamashita F, Grossmann MV, Olivato JB. Eco-friendly materials produced by blown-film extrusion as potential active food packaging. *Polym Adv Technol*. 2020;32(2):779-788.
39. Nasrin R, Biswas S, Rashid TU, et al. Preparation of chitosan-PLA laminated composite for implantable application. *Bioactive Mater*. 2017;2(4):199-207.
40. Li J, Li J, Feng D, Zhao J, Sun J, Li D. Comparative study on properties of Polylactic acid nanocomposites with cellulose and chitosan nanofibers extracted from different raw materials. *J Nanomater*. 2017;2017:7193263.
41. Li G, Zhuang Y, Mu Q, Wang M. Preparation, characterization and aggregation behavior of amphiphilic chitosan derivative having poly (l-lactic acid) side chains. *Carbohydr Polym*. 2008;72(1):60-66.
42. Soni B, Mahmoud B. Chemical isolation and characterization of different cellulose nanofibers from cotton stalks. *Carbohydr Polym*. 2015;134:581-589.
43. Le Troedec M, Sedan D, Peyratout C, et al. Influence of various chemical treatments on the composition and structure of hemp fibres. *Compos A Appl Sci Manuf*. 2008;39(3):514-522.
44. Shankar S, Rhim J-W. Preparation of nanocellulose from microcrystalline cellulose: the effect on the performance and properties of agar-based composite films. *Carbohydr Polym*. 2016;135:18-26.
45. Pachuau L, Vanlalfakawma DC, Tripathi SK, Lalhlenmawia H. Muli bamboo (*Melocanna baccifera*) as a new source of microcrystalline cellulose. *J Appl Pharmaceut Sci*. 2014;4(11):87-94.
46. Chen W, Yu H, Liu Y, Hai Y, Zhang M, Chen P. Isolation and characterization of cellulose nanofibers from four plant cellulose fibers using a chemical-ultrasonic process. *Cellulose*. 2011;18(2):433-442.
47. Zheng D, Zhang Y, Guo Y, Yue J. Isolation and characterization of nanocellulose with a novel shape from walnut (*Juglans regia* L.) shell agricultural waste. *Polymer*. 2019;11(7):1130.
48. Ghasemi S, Behrooz R, Ghasemi I, Yassar RS, Long F. Development of nanocellulose-reinforced PLA nanocomposite by using maleated PLA (PLA-g-MA). *J Thermoplast Compos Mater*. 2018;31(8):1090-1101.
49. Lee S-Y, Mohan DJ, Kang I-A, Doh G-H, Lee S, Han SO. Nanocellulose reinforced PVA composite films: effects of acid treatment and filler loading. *Fibers Polym*. 2009;10(1):77-82.
50. Murphy CA, Collins MN. Microcrystalline cellulose reinforced polylactic acid biocomposite filaments for 3D printing. *Polym Compos*. 2018;39(4):1311-1320.
51. Olaiya NG, Surya I, Oke P, et al. Properties and characterization of a PLA–chitosan–starch biodegradable polymer composite. *Polymer*. 2019;11(10):1656.
52. Coltelli M-B, Cinelli P, Gigante V, et al. Chitosan nanofibrils in poly (lactic acid)(PLA) nanocomposites: dispersion and thermo-mechanical properties. *Int J Mol Sci*. 2019;20(3):504.
53. Yang Z, Li X, Si J, Cui Z, Peng K. Morphological, mechanical and thermal properties of poly (lactic acid)(PLA)/cellulose nanofibrils (CNF) composites nanofiber for tissue engineering. *J Wuhan Univ Technol Mater Sci Ed*. 2019;34(1):207-215.
54. Surya I, Olaiya NG, Rizal S, et al. Plasticizer enhancement on the miscibility and thermomechanical properties of Polylactic acid-chitosan-starch composites. *Polymer*. 2020;12(1):115.

How to cite this article: Nasution H, Olaiya NG, Haafiz MKM, et al. The role of amphiphilic chitosan in hybrid nanocellulose–reinforced polylactic acid biocomposite. *Polym Adv Technol*. 2021;1–12. https://doi.org/10.1002/pat.5355